Dimension Reduction for Efficient Data-Enabled Predictive Control

Kaixiang Zhang, Yang Zheng, *Member, IEEE*, Chao Shang, *Member, IEEE*, and Zhaojian Li, *Senior Member, IEEE*

***Abstract*—In this letter, we propose a simple yet effective singular value decomposition (SVD) based strategy to reduce the optimization problem dimension in data-enabled predictive control (DeePC). Specifically, in the case of linear time-invariant systems, the excessive input/output measurements can be rearranged into a smaller data library for the non-parametric representation of system behavior. Based on this observation, we develop an SVD-based strategy to pre-process the offline data that achieves dimension reduction in DeePC. Numerical experiments confirm that the proposed method significantly enhances the computation efficiency without sacrificing the control performance.**

***Index Terms*—Data-driven control, dimension reduction, predictive control.**

I. Introduction

With advancement in computing and sensing technologies, data-driven control approaches have become increasingly prevalent in the context of complex dynamic systems [1], [2]. When modeling based on first-principles is infeasible or too costly, data-driven control approaches can circumvent explicit system models and directly incorporate collected data for control development, offering an appealing alternative to classical model-based methods [1].

Recent developments in data-driven model predictive control (MPC) have shown great promise to achieve optimal control with simultaneous constraint satisfaction and stability guarantees [3], [4]. Particularly, Data-EnablEd Predictive Control (DeePC) [5] receives increasing attention as it can directly exploit input/output data to achieve safe and optimal control of unknown systems. In contrast to conventional MPC schemes that depend on explicit parametric models, DeePC leverages Willems' fundamental lemma [6] to represent system trajectories in a non-parametric manner. Specifically, the fundamental lemma shows that a data Hankel matrix consisting of a pre-collected input/output trajectory of a linear system spans the vector space of all trajectories that the system can produce, given that the input sequence is persistently exciting [6]. This lemma plays an essential role in DeePC and has been applied to tackle various control problems [2], [7], [8], [9]; see [1] for an extensive review. DeePC has found success across diverse applications, including quadcopters [10], power systems [11], [12], and connected and autonomous vehicles [13], [14].

All the aforementioned applications show the value of the fundamental lemma and the potential of the DeePC method. Yet, a major challenge in DeePC is the high computational complexity; at each iteration, it needs to solve an optimization problem with high-dimensional variables, which might be computationally intractable in resource-limited situations. In particular, to implement DeePC, sufficiently rich input/output data should be recorded offline, and then the Hankel matrix is used to store the data for the non-parametric representation of unknown systems. Since the dimension of optimization variables in DeePC is determined by the length of pre-collected data, excessive up-front data collection will lead to overly high optimization dimensions in the subsequent online calculation. For real-time implementation in resource-limited situations, it is necessary to reformulate (and possibly approximate) the original optimization problem in DeePC to reduce the dimension of optimization variables for efficient computation.

In this letter, we introduce a *minimum-dimension* version of the DeePC method, which admits significantly better computational efficiency with no/little degradation in control performance. The idea is based on a well-known observation that the Hankel matrix in the fundamental lemma is always *low-rank*. Thus, a new data matrix with a smaller column dimension could be constructed to represent the system input/output behavior, which balances the tradeoff between control performance and computational complexity. Based on this observation, we develop a singular value decomposition (SVD) based strategy to extract the principal components from a large data library (i.e., the Hankel matrix). The resulting smaller data library is then incorporated into DeePC, which effectively reduces the dimension of optimization variables. We denote this new formulation as minimum-dimension DeePC, since the dimension of optimization variables becomes minimal to represent the system behavior.

Manuscript received 23 June 2023; revised 31 August 2023; accepted 23 September 2023. Date of publication 9 October 2023; date of current version 25 October 2023. This work was supported in part by the National Science Foundation (NSF) under Grant CMMI-2320698 and Grant CMMI-2320697. The work of Yang Zheng was supported in part by NSF under Grant ECCS-2154650. Recommended by Senior Editor A. P. Aguiar. *(Corresponding author: Zhaojian Li.)*

Kaixiang Zhang and Zhaojian Li are with the Department of Mechanical Engineering, Michigan State University, East Lansing, MI 48824 USA (e-mail: zhangk64@msu.edu; lizhaoj1@msu.edu).

Yang Zheng is with the Department of Electrical and Computer Engineering, University of California at San Diego, La Jolla, CA 92093 USA (e-mail: zhengy@eng.ucsd.edu).

Chao Shang is with the Department of Automation, Tsinghua University, Beijing 100084, China (e-mail: c-shang@tsinghua.edu.cn).

Digital Object Identifier 10.1109/LCSYS.2023.3322965

We note that the SVD-based technique was utilized in [15] as a heuristic to reduce the dimension of the Hankel matrix, but there was no analysis to justify the design. In this letter, the rationale behind using SVD for dimension reduction is formalized, and the conclusions are generalizable to other forms of data matrices (e.g., Page matrix and mosaic-Hankel matrix). In addition, similar SVD-based strategies have been used in data-driven control [1], [5], [11] and system identification [16], [17] but with different purposes. Specifically, the studies [1], [5], [11], [16], [17] use SVD to get a low-rank matrix approximation for the sake of denoising, while we aim to attain reduced-dimensional problems for the purpose of efficient computation. Thus, the Hankel matrix after the SVD pre-processing in [1], [5], [11], [16], [17] still remains the same size, while our SVD-based strategy reduces the dimension of the Hankel matrix significantly. Extensive simulations validate the performance of our SVD-based strategy for DeePC and confirm the benefits of improving numerical efficiency without compromising the control performance.

Notation: We use $0_{n\times m}$ and I_n to denote a zero matrix of size $n \times m$ and an $n \times n$ identity matrix, respectively. Given a signal $\omega(t) \in \mathbb{R}^n$ and two integers $i, j \in \mathbb{Z}$ with $i \le j$, we denote by $\omega_{[i,j]}$ the restriction of $\omega(t) \in \mathbb{R}^n$ to the interval $[i, j]$, namely, $\omega_{[i,j]} := \left[\omega^\mathsf{T}(i), \omega^\mathsf{T}(i+1), \dots, \omega^\mathsf{T}(j)\right]^\mathsf{T}$. To simplify notation, we also use $\omega_{[i,j]}$ to denote the sequence $\{\omega(i), \dots, \omega(j)\}$. The Hankel matrix of depth $k \in \mathbb{Z}$ ($k \le j-i+1$) associated with $\omega_{[i,j]}$ is defined as

$$\mathcal{H}_k(\omega_{[i,j]}) := \begin{bmatrix} \omega(i) & \omega(i+1) & \cdots & \omega(j-k+1) \\ \omega(i+1) & \omega(i+2) & \cdots & \omega(j-k+2) \\ \vdots & \vdots & \ddots & \vdots \\ \omega(i+k-1) & \omega(i+k) & \cdots & \omega(j) \end{bmatrix}.$$

Definition 1: The sequence $\omega_{[i,j]}$ is said to be *persistently exciting of order* k if $\mathcal{H}_k(\omega_{[i,j]})$ has full row rank of nk.

II. Preliminaries

In this section, we overview a non-parametric representation of linear systems [6] and the DeePC formulation [5].

A. Non-Parametric Representation of Linear Systems

Consider a discrete-time linear time-invariant (LTI) system

$$\begin{aligned} x(t+1) &= Ax(t) + Bu(t), \\ y(t) &= Cx(t) + Du(t), \end{aligned} \tag{1}$$

where $A \in \mathbb{R}^{n\times n}$, $B \in \mathbb{R}^{n\times m}$, $C \in \mathbb{R}^{p\times n}$, $D \in \mathbb{R}^{p\times m}$ are system matrices, and $x(t) \in \mathbb{R}^n$, $u(t) \in \mathbb{R}^m$, and $y(t) \in \mathbb{R}^p$ denote the state, control input, and output, respectively.

Model (1) is a parametric description of the system, defined by (A, B, C, D). Willems' fundamental lemma allows us to represent (1) via a finite collection of its input/output data. Let $(u^{\mathrm{d}}_{[0,\ T-1]}, y^{\mathrm{d}}_{[0,\ T-1]})$ be a length-T input/output trajectory of system (1). The Hankel matrices $\mathcal{H}_L(u^{\mathrm{d}}_{[0,\ T-1]})$ and $\mathcal{H}_L(y^{\mathrm{d}}_{[0,\ T-1]})$ are given by

$$\begin{bmatrix} \mathcal{H}_L(u^{\mathrm{d}}_{[0,\ T-1]}) \\ \hline \mathcal{H}_L(y^{\mathrm{d}}_{[0,\ T-1]}) \end{bmatrix} := \left[\begin{array}{cccc} u^{\mathrm{d}}(0) & u^{\mathrm{d}}(1) & \cdots & u^{\mathrm{d}}(T-L) \\ \vdots & \vdots & & \vdots \\ u^{\mathrm{d}}(L-1) & u^{\mathrm{d}}(L) & \cdots & u^{\mathrm{d}}(T-1) \\ \hline y^{\mathrm{d}}(0) & y^{\mathrm{d}}(1) & \cdots & y^{\mathrm{d}}(T-L) \\ \vdots & \vdots & & \vdots \\ y^{\mathrm{d}}(L-1) & y^{\mathrm{d}}(L) & \cdots & y^{\mathrm{d}}(T-1) \end{array}\right], \tag{2}$$

where each column is a length-L input/output trajectory of (1). The column space gives a non-parametric representation of (1) when the input sequence is persistently exciting as shown in the following lemma.

Lemma 1 (Fundamental Lemma [2], [6]): Consider a controllable LTI system (1) and assume that the input sequence $u^{\mathrm{d}}_{[0,\ T-1]}$ is persistently exciting of order $n+L$. Then, any length-L sequence $(u_{[0,L-1]}, y_{[0,L-1]})$ is an input/output trajectory of (1) if and only if we have

$$\begin{bmatrix} u_{[0,\ L-1]} \\ y_{[0,\ L-1]} \end{bmatrix} = \begin{bmatrix} \mathcal{H}_L(u^{\mathrm{d}}_{[0,\ T-1]}) \\ \mathcal{H}_L(y^{\mathrm{d}}_{[0,\ T-1]}) \end{bmatrix} g \tag{3}$$

for some real vector $g \in \mathbb{R}^{T-L+1}$.

B. Data-EnablEd Predictive Control

Conventional control strategies rely on the explicit system model (A, B, C, D) in (1) to facilitate the controller design, while DeePC [5], [1, Sec. 5.2] is a non-parametric approach which bypasses system identification and directly utilizes pre-collected input/output data to design a safe control policy. In particular, DeePC employs pre-collected data to predict the system behavior based on the fundamental lemma.

Let $T_{\mathrm{ini}}, N \in \mathbb{Z}$, and $L = T_{\mathrm{ini}} + N$. We choose a sufficiently long input sequence $u^{\mathrm{d}}_{[0,\ T-1]}$ of length T, which is persistently exciting of order $n+L$. Let $y^{\mathrm{d}}_{[0,\ T-1]}$ be the corresponding output sequence. We divide the Hankel matrices $\mathcal{H}_L(u^{\mathrm{d}}_{[0,\ T-1]})$ and $\mathcal{H}_L(y^{\mathrm{d}}_{[0,\ T-1]})$ into the two parts (i.e., "past data" of length T_{ini} and "future data" of length N):

$$\begin{bmatrix} U_{\mathrm{p}} \\ U_{\mathrm{f}} \end{bmatrix} = \mathcal{H}_L(u^{\mathrm{d}}_{[0,\ T-1]}), \quad \begin{bmatrix} Y_{\mathrm{p}} \\ Y_{\mathrm{f}} \end{bmatrix} = \mathcal{H}_L(y^{\mathrm{d}}_{[0,\ T-1]}), \tag{4}$$

where U_{p} and U_{f} denote the first T_{ini} block rows and the last N block rows of $\mathcal{H}_L(u^{\mathrm{d}}_{[0,\ T-1]})$, respectively (similarly for Y_{p} and Y_{f}). Let $u_{\mathrm{ini}} = u_{[t-T_{\mathrm{ini}},t-1]}$ be the control input sequence within a past time horizon of length T_{ini}, and $u = u_{[t,t+N-1]}$ be the control input sequence within a prediction horizon of length N (similarly for y_{ini} and y). The DeePC solves the following constrained optimization problem at time step t:

$$\begin{aligned} \min_{g,u,y,\sigma_u,\sigma_y} \quad & \|y - y_r\|_Q^2 + \|u\|_R^2 + \lambda_u\|\sigma_u\|_2^2 + \lambda_y\left\|\sigma_y\right\|_2^2 + \lambda_g\|g\|_2^2 \\ \text{subject to} \quad & \begin{bmatrix} U_{\mathrm{p}} \\ U_{\mathrm{f}} \\ Y_{\mathrm{p}} \\ Y_{\mathrm{f}} \end{bmatrix} g = \begin{bmatrix} u_{\mathrm{ini}} \\ u \\ y_{\mathrm{ini}} \\ y \end{bmatrix} + \begin{bmatrix} \sigma_u \\ 0 \\ \sigma_y \\ 0 \end{bmatrix}, u \in \mathcal{U}, y \in \mathcal{Y}, \end{aligned} \tag{5}$$

where $y_r = \left[y_r^\mathsf{T}(t), y_r^\mathsf{T}(t+1), \dots, y_r^\mathsf{T}(t+N-1)\right]^\mathsf{T}$ is a reference trajectory, $Q \in \mathbb{S}_+^{pN}$, $R \in \mathbb{S}_+^{mN}$ are weighting matrices, $\mathcal{U}$, $\mathcal{Y}$ represent the input and output constraints, respectively, $\sigma_u \in \mathbb{R}^{mT_{\mathrm{ini}}}$, $\sigma_y \in \mathbb{R}^{pT_{\mathrm{ini}}}$ are auxiliary variables, and $\lambda_u \ge 0$, $\lambda_y \ge 0$, $\lambda_g \ge 0$ are regularization parameters.

DeePC solves (5) in a receding horizon fashion. After computing the optimal sequence $u^* = \left[u_0^{*\mathsf{T}} \ \cdots \ u_{N-1}^{*\mathsf{T}}\right]^\mathsf{T}$, we apply $(u(t), \ldots, u(t+l-1)) = (u_0^*, \ldots, u_{l-1}^*)$ to the system for some $l < N$ steps. Then, when time is shifted to $t+l$, $(u_{\text{ini}}, y_{\text{ini}})$ is updated to the most recent input/output data; see [5], [8] for more details.

Remark 1 (Dimension of g in DeePC): To guarantee the persistent excitation of the sequence $u^{\text{d}}_{[0,\ T-1]}$, the column number of the Hankel matrix $\mathcal{H}_{n+L}(u^{\text{d}}_{[0,\ T-1]})$ must be at least no less than its row number. This implies that the number of data points T must at least satisfy $T-(n+L)+1 \geq m(n+L)$, i.e., $T \geq (m+1)(n+L)-1$. Therefore, the dimension of g in (5) is lower bounded as

$$T - L + 1 \geq mL + (m+1)n, \tag{6}$$

where $L = T_{\text{ini}} + N$. Thus, a large T leads to a high dimension of the optimization variable g in (5), which increases the computation burden and thus hinders the deployment of DeePC in resource-limited situations.

Remark 2 (Practical Choice of T): In (5), the value of T_{ini} needs to be larger than the observability index[1] in order to estimate the system initial state x_{ini} at time step t [5, Lemma 4.1], [1, Lemma 1]. This observability index (upper bounded by n) and the system internal state dimension n may be unknown when the system model (1) is unknown. In practical applications, one would need to collect a sufficiently large amount of data points to satisfy $T \geq (m+1)(n+L)-1$ with $L = T_{\text{ini}} + N$ [10], [11], [13], [14]. This choice typically leads to a very large value of T, making the optimization problem (5) large-scale and nontrivial to solve efficiently.

III. Minimum-Dimension DeePC

In this section, we observe that the Hankel matrix (2) is always low-rank. This observation allows us to use a smaller data matrix to represent the input/output behavior of system (1), which can be viewed as a *minimum-dimension* version of the fundamental lemma. We then introduce a procedure based on the singular-value decomposition (SVD) of the Hankel matrix (2) to formulate a *minimum-dimension* version of DeePC, addressing the dimension issues in both Remarks 1 and 2.

A. Minimum-Dimension Fundamental Lemma

The fundamental lemma plays an essential role in the standard DeePC (5). Indeed, each column of the Hankel matrix (2) is a length-L trajectory of system (1), which can be regarded as a motion primitive. Lemma 1 guarantees that any length-L trajectory can be constructed via a linear combination of these motion primitives when the input sequence is persistently exciting. Note that the Hankel matrix

$$\mathcal{H}_L = \begin{bmatrix} \mathcal{H}_L(u^{\text{d}}_{[0,\ T-1]}) \\ \mathcal{H}_L(y^{\text{d}}_{[0,\ T-1]}) \end{bmatrix} \in \mathbb{R}^{(m+p)L\times(T-L+1)}$$

is always low-rank, meaning that many motion primitives in the columns of (2) are redundant. We can thus use less, more representative motion primitives to represent the input-output behavior of system (1).

Lemma 2: Consider a controllable LTI system (1) and assume that the input sequence $u^{\text{d}}_{[0,\ T-1]}$ is persistently exciting of order $n+L$. The following statements hold:

1) The rank of the Hankel matrix (2) satisfies

$$r := \operatorname{rank}\left(\begin{bmatrix} \mathcal{H}_L(u^{\text{d}}_{[0,\ T-1]}) \\ \mathcal{H}_L(y^{\text{d}}_{[0,\ T-1]}) \end{bmatrix}\right) \leq mL + n. \tag{7}$$

2) Suppose $\bar{\mathcal{H}}_L \in \mathbb{R}^{(m+p)L\times r}$ has the same range space with the Hankel matrix (2). Then, any length-L sequence $(u_{[0,\ L-1]}, y_{[0,\ L-1]})$ is an input/output trajectory of (1) if and only if we have

$$\begin{bmatrix} u_{[0,\ L-1]} \\ y_{[0,\ L-1]} \end{bmatrix} = \bar{\mathcal{H}}_L \bar{g} \tag{8}$$

for some real vector $\bar{g} \in \mathbb{R}^r$.

This result is known in the literature (see e.g., [1, Appendix A]), but, to our knowledge, has not been utilized in reformulating DeePC to reduce the dimension for improved computational complexity. We give a brief proof of Lemma 2 below by observing the following relationship

$$\begin{bmatrix} \mathcal{H}_L(u^{\text{d}}_{[0,\ T-1]}) \\ \mathcal{H}_L(y^{\text{d}}_{[0,\ T-1]}) \end{bmatrix} = \begin{bmatrix} I_{mL} & 0_{mL\times n} \\ \mathcal{T}_L & \mathcal{O}_L \end{bmatrix} \begin{bmatrix} \mathcal{H}_L(u^{\text{d}}_{[0,\ T-1]}) \\ \mathcal{H}_1(x^{\text{d}}_{[0,\ T-L]}) \end{bmatrix}, \tag{9}$$

where the convolution matrix $\mathcal{T}_L \in \mathbb{R}^{pL\times mL}$ and the extended observability matrix $\mathcal{O}_L \in \mathbb{R}^{pL\times n}$ with L block rows are

$$\mathcal{T}_L := \begin{bmatrix} D & 0 & 0 & \cdots & 0 \\ CB & D & 0 & \cdots & 0 \\ CAB & CB & D & \cdots & 0 \\ \vdots & \vdots & \vdots & \ddots & \vdots \\ CA^{L-2}B & CA^{L-3}B & CA^{L-4}B & \cdots & D \end{bmatrix}, \mathcal{O}_L := \begin{bmatrix} C \\ CA \\ CA^2 \\ \vdots \\ CA^{L-1} \end{bmatrix},$$

and $\mathcal{H}_1(x^{\text{d}}_{[0,\ T-L]}) = \left[x^{\text{d}}(0), \ldots, x^{\text{d}}(T-L)\right]$. The factor

$$\begin{bmatrix} I_{mL} & 0_{mL\times n} \\ \mathcal{T}_L & \mathcal{O}_L \end{bmatrix} \in \mathbb{R}^{(m+p)L\times(mL+n)}$$

in (9) has at most rank $mL+n$. We thus have the rank result (7). When L is larger than the observability index (i.e., $\operatorname{rank}(\mathcal{O}_L) = n$), the rank result in (7) can achieve the equality, i.e., $r = mL + n$. It is clear that the statement (8) is equivalent to the statement (3). We note that the matrix $\bar{\mathcal{H}}_L$ in (8) *does not need to have a Hankel structure* as the matrix in (2), as long as they have the same range space. Finally, Lemma 2 can be extended to other matrix structures such as Page matrix [8], [11] and mosaic-Hankel matrix [18]; we present the details in the Appendix of our technical report [19].

Remark 3 (Mini. Dimension of the Fundamental Lemma): The Hankel matrix (2) in Lemma 1 has $T-L+1$ motion primitives, while in Lemma 2, the number of motion primitives in $\bar{\mathcal{H}}_L$ has been reduced to $r \leq mL + n$. This upper bound is inherent to system dimensions and independent of the data length T. We can show from (6) that $T-L+1-r \geq mn$, i.e., the dimension reduction is at least mn. It is clear that the column dimension of $\bar{\mathcal{H}}_L$ is minimum in order to guarantee the behavior representation of system (1) under the persistency excitation of the input $u^{\text{d}}_{[0,\ T-1]}$. Thus, (8) can be viewed as a minimum-dimension version of Lemma 1.

Remark 4 (SVD-Based Dimension Reduction): A standard way to generate $\bar{\mathcal{H}}_L \in \mathbb{R}^{(m+p)L\times r}$ is based on the SVD of the Hankel matrix (2). In particular, we let

$$\begin{bmatrix} \mathcal{H}_L(u^{\text{d}}_{[0,\ T-1]}) \\ \mathcal{H}_L(y^{\text{d}}_{[0,\ T-1]}) \end{bmatrix} = \underbrace{\begin{bmatrix} W_1 & W_2 \end{bmatrix}}_{W} \underbrace{\begin{bmatrix} \Sigma_1 & 0 \\ 0 & 0 \end{bmatrix}}_{\Sigma} \underbrace{\begin{bmatrix} V_1 & V_2 \end{bmatrix}^{\mathsf{T}}}_{V^{\mathsf{T}}}, \tag{10}$$

[1]The smallest integer l such that $\left[C^{\mathsf{T}}, (CA)^{\mathsf{T}}, \ldots, (CA^{l-1})^{\mathsf{T}}\right]^{\mathsf{T}}$ has full column rank n.

where $WW^{\top} = W^{\top}W = I_{(m+p)L}$ and $VV^{\top} = V^{\top}V = I_{T-L+1}$, and $\Sigma_1 \in \mathbb{R}^{r\times r}$ contains the top r non-zero singular values. The choice

$$\bar{\mathcal{H}}_L = \mathcal{H}_L V_1 = W_1\Sigma_1 \in \mathbb{R}^{(m+p)L\times r} \tag{11}$$

satisfies the range space condition in Lemma 2.

B. Minimum-Dimension DeePC

After collecting the input/output data sequences $u^{\mathrm{d}}_{[0,\ T-1]}$, $y^{\mathrm{d}}_{[0,\ T-1]}$ and forming the Hankel data matrices in (4), we can apply the SVD technique in Remark 4 to compute a new data library $\bar{\mathcal{H}}_L \in \mathbb{R}^{(m+p)L\times r}$ in (11) and consequently achieve dimension reduction in DeePC.

In particular, we replace the DeePC problem in (5) by

$$\min_{\bar{g},u,y,\sigma_u,\sigma_y} \ \|y-y_r\|_Q^2 + \|u\|_R^2 + \lambda_u\|\sigma_u\|_2^2 + \lambda_y\|\sigma_y\|_2^2 + \lambda_g\|\bar{g}\|_2^2$$

$$\text{subject to} \quad \bar{\mathcal{H}}_L\bar{g} = \begin{bmatrix} u_{\mathrm{ini}} \\ u \\ y_{\mathrm{ini}} \\ y \end{bmatrix} + \begin{bmatrix} \sigma_u \\ 0 \\ \sigma_y \\ 0 \end{bmatrix}, u \in \mathcal{U}, y \in \mathcal{Y}. \tag{12}$$

We refer to (12) as the *minimum-dimension* version of DeePC, since the column dimension of $\bar{\mathcal{H}}_L$ is minimum to guarantee the behavior representation of LTI systems. The optimization variable g in (5) has a dimension of $T-L+1$, while in (12), the dimension of the optimization variable $\bar{g}$ has been reduced to r. As discussed in Remark 3, the dimension reduction holds a lower bound of mn, which can be significant when the system has a large internal system state dimension n or input dimension m. In addition, the dimension reduction scheme assumes a prominent role in practical applications (e.g., [10], [11], [13], [14]), especially when the value of n and the bound on T_{ini} are unknown and T needs to be sufficiently large as discussed in Remark 2.

It is not difficult to see that the objective functions in (5) and (12) are strongly convex when $\lambda_u > 0, \lambda_y > 0, \lambda_g > 0$. Both (5) and (12) have a unique optimal solution if $u \in \mathcal{U}, y \in \mathcal{Y}$ are convex constraints. Indeed, we can show the equivalence of the unique optimal solution $(u^*, y^*, \sigma_u^*, \sigma_y^*)$ for (5) and (12).

Theorem 1: Suppose $\bar{\mathcal{H}}_L$ is generated with (11) that shares the same range space with $\mathcal{H}_L$, the parameters λ_u, λ_y, and λ_g are positive, and $\mathcal{U}$ and $\mathcal{Y}$ are convex polytopes. If g^* minimizes (5), then $\bar{g}^* = V_1^{\top}g^*$ is the minimizer of (12). Moreover, (5) and (12) have the same optimal solution $(u^*, y^*, \sigma_u^*, \sigma_y^*)$.

The proof details are postponed to the Appendix. The idea is to utilize the KKT condition of (5) and (12) to establish the connection between g^* and $\bar{g}^*$. We note that the polyhedral constraints $\mathcal{U}$ and $\mathcal{Y}$ allow simple KKT conditions. Then, leveraging matrix properties obtained through SVD in (10), we prove the equivalence of the optimal solution $(u^*, y^*, \sigma_u^*, \sigma_y^*)$ between (5) and (12).

Remark 5 (Cases Beyond Deterministic LTI Systems): One main motivation of the regularization in (5) is to handle systems beyond deterministic LTI with measurement and process noises [5, Sec. VI] (see [1], [8] for more details). In this case, the Hankel matrix (2) is typically full rank. However, it is unnecessary and not beneficial to use the full range space of the Hankel matrix in (5) (which is one main reason for using regularization on σ_u, σ_y, and g to select important columns). In this case, we can still use SVD-based techniques to extract the dominant range space of the Hankel matrix (2). In particular, after performing SVD (10), we plot singular values in Σ by using a base-10 logarithmic scale. Via the distribution of singular values in descending order, an appropriate selection of r can be informed by the turning point, which indicates the transition from singular values/vectors that represent principal patterns to those that are insignificant. This leads to a much condensed data library $\bar{\mathcal{H}}_L \in \mathbb{R}^{(m+p)L\times r}$ with a reduced column number. This strategy is generally robust to the length T of the input sequence $u^{\mathrm{d}}_{[0,\ T-1]}$. In practice, the length T can be chosen as large as possible, but the value of r via SVD may still remain small. This addresses the dimension issue in Remark 2.

IV. Numerical Experiments

This section presents two numerical examples to demonstrate the effectiveness of our SVD-based approach. All computations are performed in MATLAB 2022a on a laptop with an Intel i7-10710U CPU with 6 cores, 1.6 GHz clock rate and 16 GB RAM. The DeePC problem can be transformed into the quadratic problem and is solved with the MATLAB function `quadprog`.

A. Linear System Case Study

We first consider an LTI system with matrices (A, B, C, D) as follows

$$A = \begin{bmatrix} 0.921 & 0 & 0.041 & 0 \\ 0 & 0.918 & 0 & 0.033 \\ 0 & 0 & 0.924 & 0 \\ 0 & 0 & 0 & 0.937 \end{bmatrix}, B = \begin{bmatrix} 0.017 & 0.001 \\ 0.001 & 0.023 \\ 0 & 0.061 \\ 0.072 & 0 \end{bmatrix},$$

$$C = \begin{bmatrix} 1 & 0 & 0 & 0 \\ 0 & 1 & 0 & 0 \end{bmatrix}, D = 0_{2\times 2}.$$

The control objective is to track the setpoint $y_r(t) = \left[0.65, 0.77\right]^{\top}$, and the input/output constraints are $\left[-2, -2\right]^{\top} \le u(t) \le \left[2, 2\right]^{\top}$ and $\left[-2, -2\right]^{\top} \le y(t) \le \left[2, 2\right]^{\top}$, respectively.

In an offline experiment, an input/output trajectory of length $T = 400$ is collected, where the input $u(t)$ is chosen randomly from $\left[-3, 3\right]^{\top}$, and the output $y(t)$ are subject to uniformly distributed noise over $\left[-0.002, 0.002\right]^{\top}$. The time horizons for the previous data sequence and future data sequence are chosen as $T_{\mathrm{ini}} = 10$ and $N = 20$, and thus $L = T_{\mathrm{ini}} + N = 30$. The weighting matrices Q, R and the regularization parameters λ_u, λ_y, λ_g are chosen as $Q = 35\cdot I_{40}$, $R = 10^{-4}I_{40}$, $\lambda_u = 10^6$, $\lambda_y = 10^4$, and $\lambda_g = 10^2$, respectively. We can calculate that the Hankel matrix $\mathcal{H}_L$ is of size 120×371, while its rank should be at most $mL + n = 64$ under the noise-free deterministic case. The singular value distribution of $\mathcal{H}_L$ (i.e., σ_i, $i = 1, \ldots, 120$) is shown in Fig. 1. It is clear that the turning point is 64, which is consistent with the analysis.

We extract the first $r = 64$ columns and singular values from W and Σ, respectively, to construct $\bar{\mathcal{H}}_L$ as discussed in Remark 4. For comparison, the original data library $\mathcal{H}_L$, its direct truncation matrix $\mathcal{H}_{L,[1:r]}$ (i.e., the first r columns of $\mathcal{H}_L$ are extracted to construct the truncation matrix), and the new data library $\bar{\mathcal{H}}_L$ are used in DeePC. Fig. 2 shows the simulation results. It is clear that both the original data library $\mathcal{H}_L$ and the low-dimensional library $\bar{\mathcal{H}}_L$ can be well embedded into the DeePC framework to achieve satisfactory

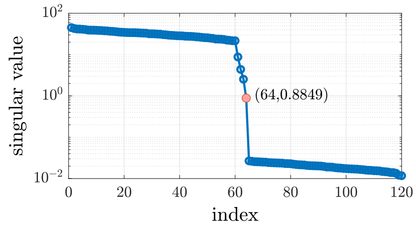

Fig. 1. Singular value distribution of $\mathcal{H}_L$ in linear system case.

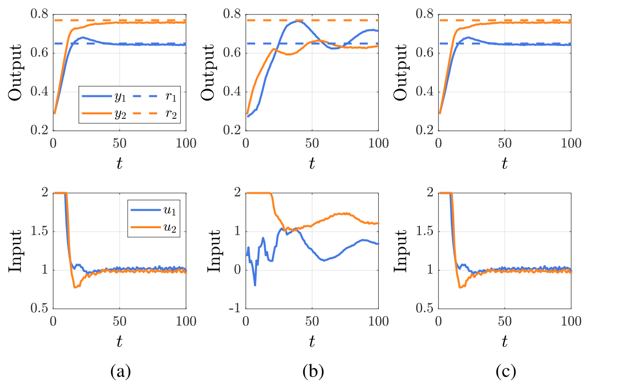

Fig. 2. Output and input evolution of the linear system, resulting from the application of the DeePC algorithm with (a) original data library $\mathcal{H}_L$, (b) truncation matrix $\mathcal{H}_{L,[1:r]}$, and (c) new data library $\bar{\mathcal{H}}_L$.

TABLE I

COMPARISON IN THE LINEAR SYSTEM CASE STUDY

	DeePC	Minimum-Dimension DeePC
Dimension of the variable $g/\bar{g}$	371	64
Average Computation Time [ms]	48.34	17.34
Accumulative Cost	169.63	169.64

control performance, while the truncation matrix $\mathcal{H}_{L,[1:r]}$ fails to regulate the output signals.

In Table I, we further list the accumulative cost (i.e., $\sum(\|y-y_r\|_Q^2 + \|u\|_R^2)$) and the average computation time per iteration of the DeePC algorithm based on $\mathcal{H}_L$ and $\bar{\mathcal{H}}_L$. Since $\bar{\mathcal{H}}_L$ has a much lower column dimension than $\mathcal{H}_L$ (64 vs. 371), its DeePC implementation admits more efficient computation (17 ms vs. 48 ms), while maintaining similar closed-loop performance thanks to the SVD procedure that extracts principle patterns.

B. Case Study With Nonlinear Traffic System

To evaluate the performance of the proposed minimum-version DeePC scheme for nonlinear systems, we consider the leading cruise control (LCC) of connected and autonomous vehicles (CAVs) in mixed traffic scenarios [13].

As shown in Fig. 3, the mixed traffic consists of $n+1$ vehicles: one head vehicle (indexed as 0), m CAVs, and $n-m$ human-driven vehicles (HDVs). Let $\Omega = \{1, 2, \ldots, n\}$ be the set of vehicle indices ordered from front to end. The sets of CAV indices and HDV indices are denoted by $\Omega_C = \{i_1, \ldots, i_m\} \subseteq \Omega$ and $\Omega_H = \{j_1, \ldots, j_{n-m}\} = \Omega \backslash \Omega_C$, respectively, where $i_1 < \ldots < i_m$ and $j_1 < \ldots < j_{n-m}$. The spacing error, velocity error and acceleration of the i-th vehicle at time t is denoted as $\tilde{s}_i(t)$, $\tilde{v}_i(t)$ and $u_i(t)$, respectively. The system state, input, and output of the mixed traffic are given by, respectively, $x(t) = \left[\tilde{s}_1(t), \tilde{v}_1(t), \ldots, \tilde{s}_n(t), \tilde{v}_n(t)\right]^{\mathsf{T}}$,

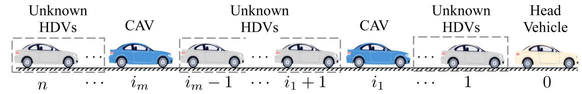

Fig. 3. Schematic of mixed traffic system with $n+1$ vehicles.

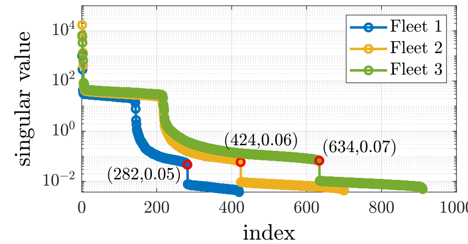

Fig. 4. Singular value distribution of $\mathcal{H}_L$ for Fleet 1, Fleet 2, and Fleet 3.

and

$$u(t) = \left[u_{i_1}(t), \ldots, u_{i_m}(t)\right]^{\mathsf{T}},$$
$$y(t) = \left[\tilde{v}_1(t), \ldots, \tilde{v}_n(t), \tilde{s}_{i_1}(t), \ldots, \tilde{s}_{i_m}(t)\right]^{\mathsf{T}}.$$

A method called the DeeP-LCC algorithm has been developed in [13] to achieve safe and optimal control of CAVs.

We test our developed approach under three fleet structures with different numbers of CAVs and HDVs. These three fleets are described by

$$\text{Fleet 1: } n = 3, m = 1, \Omega_C = \{2\}, \Omega_H = \{1, 3\},$$
$$\text{Fleet 2: } n = 5, m = 2, \Omega_C = \{2, 4\}, \Omega_H = \{1, 3, 5\},$$
$$\text{Fleet 3: } n = 8, m = 2, \Omega_C = \{3, 6\}, \Omega_H = \{1, 2, 4, 5, 7, 8\}.$$

As suggested in [13], the length for the pre-collected data is chosen as $T = 2000$, $T = 3000$, and $T = 4000$, respectively, under these three fleet structures. The remaining parameters used to set up the DeePC are selected as the same with [13]. A safety-critical scenario is considered in our simulation; see [13, Sec. VI-C] for a detailed description.

For these three fleet structures, $\mathcal{H}_L$ has a dimension of 420×1931, 700×2931, and 910×3931, respectively, and its corresponding singular values distribution is shown in Fig. 4. It is clear that the data Hankel matrices have a low rank, and accordingly, we select r as $r = 282$, $r = 424$, and $r = 634$, respectively. Under each fleet, the data library $\mathcal{H}_L$ and the low-dimensional data library $\bar{\mathcal{H}}_L$ are utilized in DeePC for the control of CAVs. We use fuel consumption, average absolute velocity error (AAVE) [13], and average computation time per iteration to depict the performance.

The results are summarized in Table II. It is noted that under different fleet structures, the proposed minimum-dimension DeePC consistently offers an order of magnitude faster computational time while achieving similar control performance as compared to the original DeePC. This confirms that, in the context of nonlinear systems, the SVD-based approach can successfully extract the principle patterns from $\mathcal{H}_L$, and thus the new data library $\bar{\mathcal{H}}_L$ preserves the critical information of $\mathcal{H}_L$, while allowing for a more efficient representation of the system behavior. Therefore, the resulting minimum-dimension DeePC can accomplish better computational efficiency without compromising the control performance.

V. CONCLUSION

This letter has presented an SVD-based strategy to reduce the dimension of the optimization problem in DeePC. It

TABLE II
COMPARISON IN THE NONLINEAR SYSTEM CASE

	DeePC	Minimum-Dimension DeePC		DeePC	Minimum-Dimension DeePC
Dimension of $g/\bar{g}$			**Average Computation Time** [s]		
Fleet 1	1931	282	Fleet 1	1.02	0.06
Fleet 2	2931	424	Fleet 2	3.59	0.25
Fleet 3	3931	634	Fleet 3	7.41	0.36
Fuel Consumption [mL]			**AAVE** $[10^{-2}]$		
Fleet 1	94.83	94.79	Fleet 1	10.77	10.78
Fleet 2	179.19	179.10	Fleet 2	14.32	14.31
Fleet 3	303.94	304.06	Fleet 3	21.39	21.40

is known that a large data library measured from an LTI system can be refined into a low-dimensional one for the non-parametric representation of system behavior. Based on this observation, we have proposed an SVD-based approach to extract the main components from the large data library and subsequently reduce the optimization problem dimension in the DeePC formulation. Simulation results showcase that by using the proposed method, the computation efficiency of the DeePC algorithm can be an order of magnitude faster without sacrificing the control performance.

APPENDIX

We here present the proof details of Theorem 1. Since $\mathcal{U}$ and $\mathcal{Y}$ are convex polytopes, we can rewrite $u \in \mathcal{U}$ and $y \in \mathcal{Y}$ as $B\left[u^\top, y^\top\right]^\top \leq c$ for some matrix B and vector c. Both (5) and (12) have unique optimal solutions since they are strongly convex. Eliminating the variables u, y, σ_u, σ_y in the DeePC (5) leads to

$$\begin{aligned} \min_{g} \quad & \|\mathcal{H}_L g - b\|_P^2 + \lambda_g \|g\|_2^2 \\ \text{subject to} \quad & Cg \leq c, \end{aligned} \tag{13}$$

where $b = \left[u_{\text{ini}}^\top, 0, y_{\text{ini}}^\top, y_r^\top\right]^\top$, P is the block-diagonal matrix $\text{blkdiag}(\lambda_u I_{mT_{\text{ini}}}, R, \lambda_y I_{pT_{\text{ini}}}, Q)$, and $C = B\left[U_f^\top, Y_f^\top\right]^\top$. Based on (13), we define the Lagrangian $\mathcal{L}(g, \mu) = \|\mathcal{H}_L g - b\|_P^2 + \lambda_g \|g\|_2^2 + \mu^\top (Cg - c)$, where μ denotes the dual variable. Let (g^*, μ^*) be the minimizer of (13). Then, it should satisfy the following KKT condition:

$$\begin{cases} 2\mathcal{H}_L^\top P(\mathcal{H}_L g^* - b) + 2\lambda_g g^* + C^\top \mu^* = 0, \\ {\mu^*}^\top (Cg^* - c) = 0, \\ Cg^* \leq c, \quad \mu^* \geq 0. \end{cases} \tag{14}$$

Similarly, (12) can be reformulated as

$$\begin{aligned} \min_{\bar{g}} \quad & \|\bar{\mathcal{H}}_L \bar{g} - b\|_P^2 + \lambda_g \|\bar{g}\|_2^2 \\ \text{subject to} \quad & \bar{C}\bar{g} \leq c, \end{aligned} \tag{15}$$

where $\bar{C} = CV_1$. The Lagrangian of (15) is in the form of $\bar{\mathcal{L}}(\bar{g}, \bar{\mu}) = \|\bar{\mathcal{H}}_L \bar{g} - b\|_P^2 + \lambda_g \|\bar{g}\|_2^2 + \bar{\mu}^\top (\bar{C}\bar{g} - c)$, where $\bar{\mu}$ denotes the dual variable. By utilizing $\bar{\mathcal{H}}_L = \mathcal{H}_L V_1$ (i.e., (11)), $\bar{C} = CV_1$ and $V_1^\top V_1 = I_r$, the KKT condition of (15) is

$$\begin{cases} V_1^\top (2\mathcal{H}_L^\top P(\mathcal{H}_L V_1 \bar{g}^* - b) + 2\lambda_g V_1 \bar{g}^* + C^\top \bar{\mu}^*) = 0, \\ \bar{\mu}^{*\top} (CV_1 \bar{g}^* - c) = 0, \\ CV_1 \bar{g}^* \leq c, \quad \bar{\mu}^* \geq 0. \end{cases} \tag{16}$$

From (10) and $C = B\left[U_f^\top, Y_f^\top\right]^\top$, we know that $V_1 V_1^\top = I_{T-L+1} - V_2 V_2^\top$, $V_1^\top V_2 = 0$, $\mathcal{H}_L V_2 = 0$, and $CV_2 = 0$. Note that (16) and these matrix properties are upheld by requiring $\bar{\mathcal{H}}_L$, generated from (11), has the same range space as $\mathcal{H}_L$.

Based on the aforementioned matrix properties and (14), it is easy to verify that $(\bar{g}^* = V_1^\top g^*, \bar{\mu}^* = \mu^*)$ satisfies the KKT condition (16). Therefore, if g^* is the minimizer of (13) (i.e., (5)), then $\bar{g}^* = V_1^\top g^*$ minimizes (15) (i.e., (12)). Finally, given $\bar{g}^* = V_1^\top g^*$, we have

$$\bar{\mathcal{H}}_L \bar{g}^* = \mathcal{H}_L (V_1 V_1^\top) g^* = \mathcal{H}_L (I_{T-L+1} - V_2 V_2^\top) g^* = \mathcal{H}_L g^*,$$

which indicates that (5) and (12) have the same unique optimal solution $(u^*, y^*, \sigma_u^*, \sigma_y^*)$.

REFERENCES

[1] I. Markovsky and F. Dörfler, "Behavioral systems theory in data-driven analysis, signal processing, and control," *Annu. Rev. Control*, vol. 52, no. 52, pp. 42–64, Nov. 2021.
[2] C. De Persis and P. Tesi, "Formulas for data-driven control: Stabilization, optimality, and robustness," *IEEE Trans. Autom. Control*, vol. 65, no. 3, pp. 909–924, Mar. 2020.
[3] U. Rosolia and F. Borrelli, "Learning model predictive control for iterative tasks. A data-driven control framework," *IEEE Trans. Autom. Control*, vol. 63, no. 7, pp. 1883–1896, Jul. 2018.
[4] L. Hewing, K. P. Wabersich, M. Menner, and M. N. Zeilinger, "Learning-based model predictive control: Toward safe learning in control," *Annu. Rev. Control Robot. Auton. Syst.*, vol. 3, no. 1, pp. 269–296, May 2020.
[5] J. Coulson, J. Lygeros, and F. Dörfler, "Data-enabled predictive control: In the shallows of the DeePC," in *Proc. 18th Eur. Control Conf.*, 2019, pp. 307–312.
[6] J. C. Willems, P. Rapisarda, I. Markovsky, and B. L. De Moor, "A note on persistency of excitation," *Syst. Control Lett.*, vol. 54, no. 4, pp. 325–329, Apr. 2005.
[7] J. Berberich, J. Köhler, M. A. Müller, and F. Allgöwer, "Data-driven model predictive control with stability and robustness guarantees," *IEEE Trans. Autom. Control*, vol. 66, no. 4, pp. 1702–1717, Apr. 2021.
[8] J. Coulson, J. Lygeros, and F. Dörfler, "Distributionally robust chance constrained data-enabled predictive control," *IEEE Trans. Autom. Control*, vol. 67, no. 7, pp. 3289–3304, Jul. 2022.
[9] S. Baros, C.-Y. Chang, G. E. Colon-Reyes, and A. Bernstein, "Online data-enabled predictive control," *Automatica*, vol. 138, Apr. 2022, Art. no. 109926.
[10] E. Elokda, J. Coulson, P. N. Beuchat, J. Lygeros, and F. Dörfler, "Data-enabled predictive control for quadcopters," *Int. J. Robust Nonlinear Control*, vol. 31, no. 18, pp. 8916–8936, Dec. 2021.
[11] L. Huang, J. Coulson, J. Lygeros, and F. Dörfler, "Decentralized data-enabled predictive control for power system oscillation damping," *IEEE Trans. Control Syst. Technol.*, vol. 30, no. 3, pp. 1065–1077, May 2022.
[12] P. Mahdavipour, C. Wieland, and H. Spliethoff, "Optimal control of combined-cycle power plants: A data-enabled predictive control perspective," *IFAC-PapersOnLine*, vol. 55, no. 13, pp. 91–96, 2022.
[13] J. Wang, Y. Zheng, K. Li, and Q. Xu, "DeeP-LCC: Data-enabled predictive leading cruise control in mixed traffic flow," *IEEE Trans. Control Syst. Technol.*, early access, Jul. 4, 2023, doi: 10.1109/TCST.2023.3288636.
[14] J. Wang, Y. Zheng, J. Dong, C. Chen, M. Cai, K. Li, and Q. Xu, "Implementation and experimental validation of data-driven predictive control for dissipating stop-and-go waves in mixed traffic," *IEEE Internet Things J.*, early access, Aug. 8, 2023, doi: 10.1109/JIOT.2023.3303039.
[15] H. Yang and S. Li, "A data-driven predictive controller design based on reduced Hankel matrix," in *Proc. 10th Asian Control Conf.*, 2015, pp. 1–7.
[16] H. Zeiger and A. McEwen, "Approximate linear realizations of given dimension via Ho's algorithm," *IEEE Trans. Autom. Control*, vol. AC-19, no. 2, pp. 153–153, Apr. 1974.
[17] A. A. H. Damen, P. M. J. Van den Hof, and A. K. Hajdasinski, "Approximate realization based upon an alternative to the Hankel matrix: The page matrix," *Syst. Control Lett.*, vol. 2, no. 4, pp. 202–208, Dec. 1982.
[18] H. J. van Waarde, C. De Persis, M. K. Camlibel, and P. Tesi, "Willems' fundamental lemma for state-space systems and its extension to multiple datasets," *IEEE Control Syst. Lett.*, vol. 4, no. 3, pp. 602–607, Jul. 2020.
[19] K. Zhang, Y. Zheng, C. Shang, and Z. Li, "Dimension reduction for efficient data-enabled predictive control," 2023, *arXiv:2211.03697*.